Catalytic Transforming Cellulose into Methane Under Natural Solar Irradiation

Yushan Yang, Shaoyu Yuan, Heli Pan, Zixuan Li, Xinlei Shen, Yongjun Gao*

Key Laboratory of Medicinal Chemistry and Molecular Diagnosis of Ministry of Education, College of Chemistry and Environmental Science, Hebei University, Baoding, 071002, China.

Corresponding author: yjgao@hbu.edu.cn

Contents

Experimental 1
Materials 1
Characterizations 2
Figure S1. The picture of instrument for the catalytic hydrogenolysis of cellulose under solar irradiation. 3
Table S1 Control experiments for cellulose hydrogenolysis. 3
Figure S2. (a) Catalytic hydrogenolysis of cellulose over Ni/SiO_2 under different hydrogen pressure. Reaction conditions: cellulose (0.15g), catalyst (0.15 g), C/Ni=10, 400 °C, 5 h. (b) Catalytic hydrogenolysis of cellulose over Ni/SiO_2 with different ratio of molar carbon in cellulose to Ni. Reaction conditions: cellulose (0.15g), 2MPa H_2, 400 °C, 5 h. (c) Cellulose hydrogenolysis over Ni/SiO_2 with different nickel content. Reaction conditions: cellulose (0.15g), C/Ni=10, 2MPa H_2, 400 °C, 5 h. 4
Figure S3. The diffuse reflectance infrared fourier transform spectra (DRIFTs) of pyridine adsorbed on different catalysts 4
Figure S4. (a) Nitrogen adsorption-desorption isotherms and (b) pore-size distribution of nickel catalyst supported on with different supports. 5
Figure S5. The signal of carbon dioxide (m/z=44) during the TPO-MS of recycled catalyst after fifth run. 6
Figure S6. The kinetic researches of the hydrogenolysis of cellulose over Ni/SiO_2 at (a) 400 °C, (b) 350 °C and (c) 300 °C. Reaction conditions: cellulose (0.15 g), catalyst (0.15 g), 2 MPa H_2 6
Table S2. The comparison with other catalytic for biomass hydrogenolysis to methane. 7
Table S3. The percentage of carbon content in natural corn straw based on elemental analysis. 8
Figure S7. The potential energies of different reaction pathway of cellulose model (containing three glucose units) on Ni(111) slab based on DFT calculations. 8
References 8

Experimental

Materials

All chemicals are of analytical grade and do not require any further pure process before they were used in the experiments. Cellulose, fumed silica, nano alumina were all purchased from Aladdin Reagent Co., Ltd. Copper nitrate was purchased from Sinopharm Co., Ltd. Ferric nitrate is produced by Tianjin Fuchen chemical reagent factory. Nickel nitrate, cobalt nitrate, nano cerium dioxide, nano hydroxyapatite and nano niobium oxide are all provided by MACKLIN reagent.

Characterizations

The powder X-ray diffraction (XRD) patterns were performed on a Bruker D8 ADVANCE diffractometer. The operating voltage, current and scan speed are set to 40 kV, 40 mA and 2θ = 4°/min, respectively. The X-ray photoelectron spectroscopy (XPS) is recorded on a Thermo ESCALAB 250XI spectrometer. The morphology and elemental mapping analysis were conducted on a transmission electron microscopy (TEM, Tecnai G2 F20).

Figure S1. The picture of instrument for the catalytic hydrogenolysis of cellulose under solar irradiation.

Table S1 Control experiments for cellulose hydrogenolysis.

Entry	**Cellulose (g)**	**Ni content in catalyst (%)**	**T (°C)**	**Time (h)**	**H_2 (MPa)**	**Residual solids (g)**	**Yield (%) CH_4**	**Yield (%) C_2H_6-C_5H_{12}**	**Yield (%) CO_2**	**C.B. (%)**
1	0.1555(cat.)	20	400	5	2	0.1555	0	0	0	0
2	CO_2 gas mixture	20	400	5	1	0	97.76	0.06	2.18	98.75
3	0.1545	20	sun	6	2	0	98.73	0.87	0.40	100
4	Butane	20	400	5	2	0	94.09	0.42	0	94.51

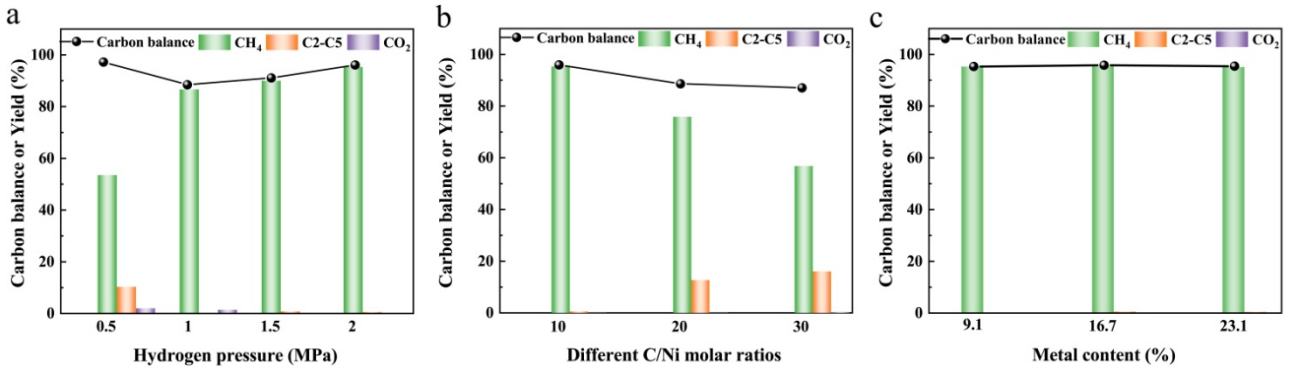

Figure S2. (a) Catalytic hydrogenolysis of cellulose over Ni/SiO_2 under different hydrogen pressure. Reaction conditions: cellulose (0.15g), catalyst (0.15 g), C/Ni=10, 400 °C, 5 h. (b) Catalytic hydrogenolysis of cellulose over Ni/SiO_2 with different ratio of molar carbon in cellulose to Ni. Reaction conditions: cellulose (0.15g), 2MPa H_2, 400 °C, 5 h. (c) Cellulose hydrogenolysis over Ni/SiO_2 with different nickel content. Reaction conditions: cellulose (0.15g), C/Ni=10, 2MPa H_2, 400 °C, 5 h.

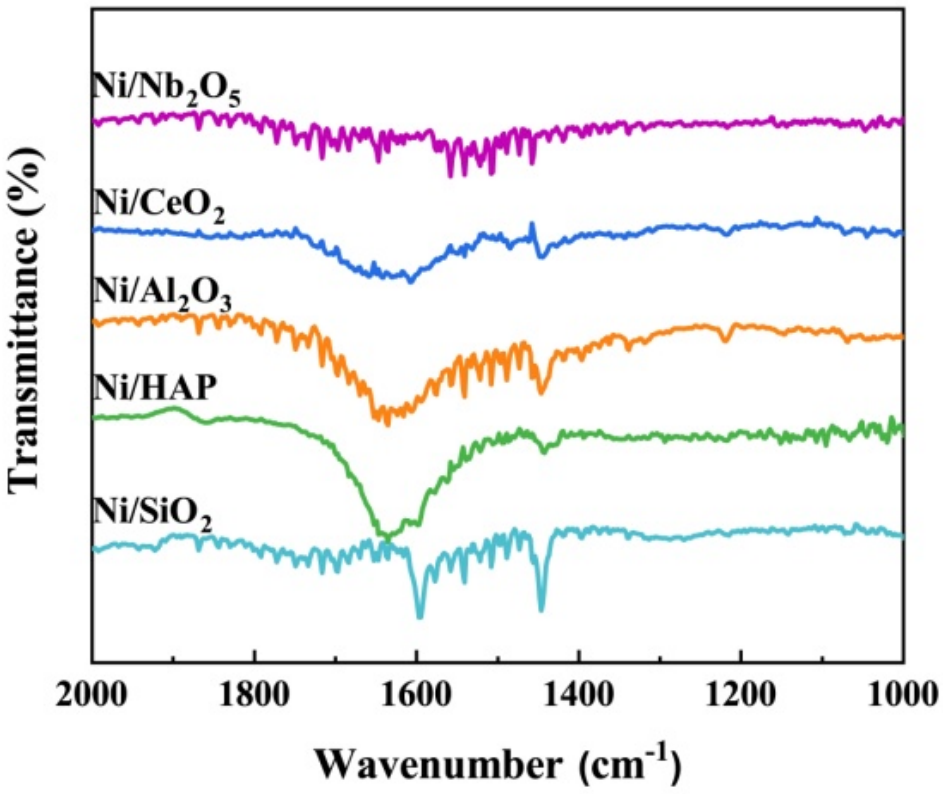

Figure S3. The diffuse reflectance infrared fourier transform spectra (DRIFTs) of pyridine adsorbed on different catalysts.

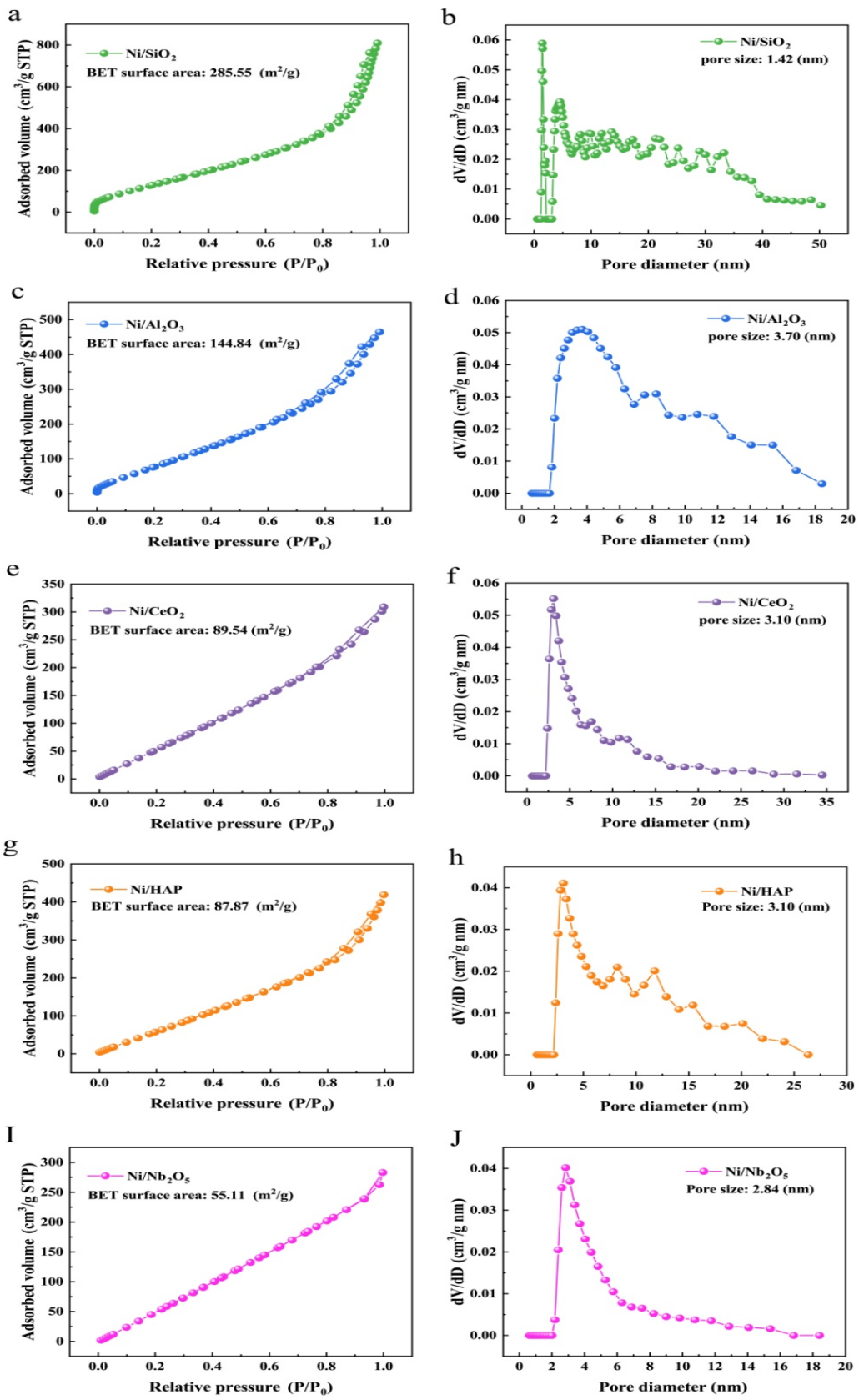

Figure S4. (a) Nitrogen adsorption-desorption isotherms and (b) pore-size distribution of nickel catalyst supported on with different supports.

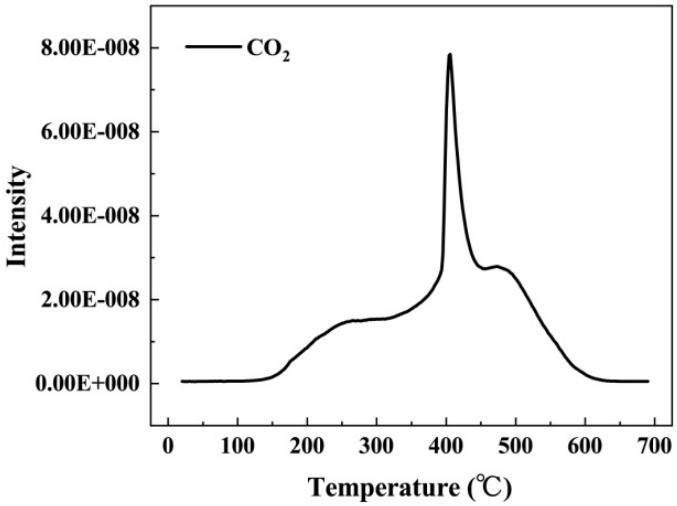

Figure S5. The signal of carbon dioxide (m/z=44) during the TPO-MS of recycled catalyst after fifth run.

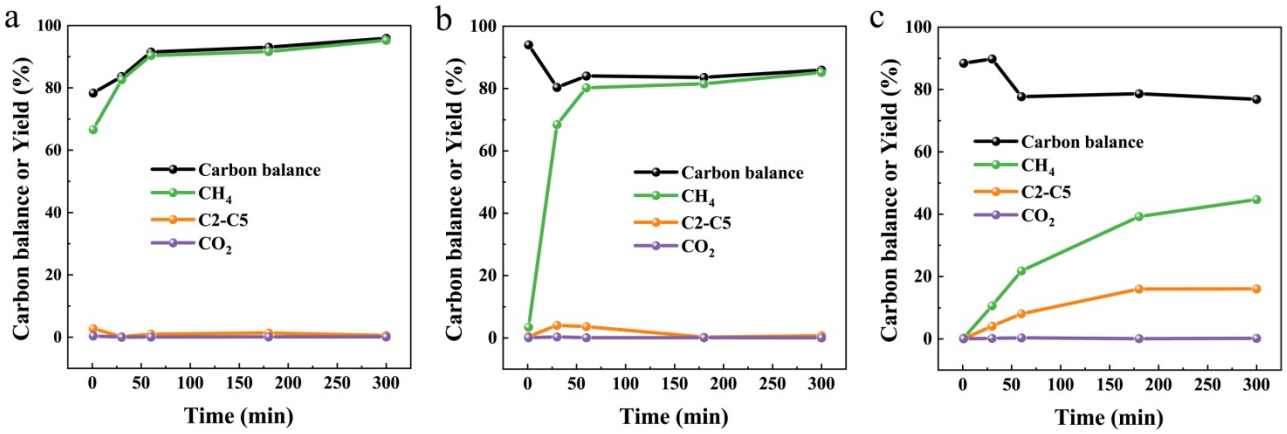

Figure S6. The kinetic researches of the hydrogenolysis of cellulose over Ni/SiO_2 at (a) 400 °C, (b) 350 °C and (c) 300 °C. Reaction conditions: cellulose (0.15 g), catalyst (0.15 g), 2 MPa H_2.

Table S2. The comparison with other catalytic for biomass hydrogenolysis to methane.

Entry	Reactant	Catalyst	T (°C)	P (MPa)	t (h)	Stir (rpm)	Solvent	Y_{CH4} (%)	Ref.
1	cellulose	Ni/SiO_2	400	2	5	-	-	96	This work
2	corn straw powder	Ni/SiO_2	400	2	10	-	-	83.65	This work
3	cellulose	Ni/SiO_2	Solar energy	2	6	-	-	98	This work
4	cellulose	5wt% Ru/C	220	1	12	800	30 mL deionized water	88.1	1
5	beech sawdust	Nickel-based alloy catalyst	300	4	5	800	20 mL of water	96	2
6	cellulose	Ru/MSN-350	250	4	5	800	20 mL of water	64	3
7	glucose	Ru/MSN-350	250	4	5	-	20 mL of water	71.5	3
8	xylan	Ru/MSN-350	250	4	5	-	20 mL of water	66	3
9	isosorbide	Ru/MSN	250	4	5	800	20 mL of wate	85.4	3
10	glycerol	Ru/Al_2O_3 + HZSM5(25)	160	8	8	800	10 mL 40 wt% glycerol	44.03	4
11	glycerol	Ru/C	200	5	2	-	10 wt.% glycerol aqueous solution	46.53	5
12	beech sawdust	Ru/P25	200	3	24	-	10 mL of H_2O	96	6

Table S3. The percentage of carbon content in natural corn straw based on elemental analysis.

Entry	Weight (mg)	C (%)
1	5.9520	41.83
2	7.6350	41.95

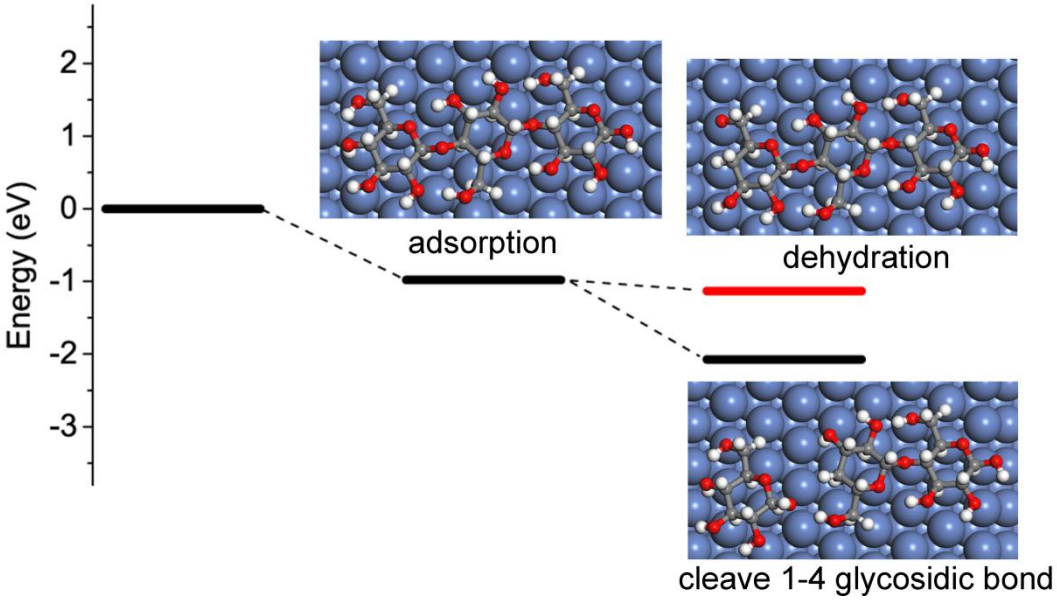

Figure S7. The potential energies of different reaction pathway of cellulose model (containing three glucose units) on Ni(111) slab based on DFT calculations.

References

1. Wang, H.; Zhang, C.; Liu, Q.; Zhu, C.; Chen, L.; Wang, C.; Ma, L., Direct Hydrogenolysis of Cellulose into Methane under Mild Conditions. *Energy & Fuels* **2018,** *32* (11), 11529-11537.
2. Si, X.; Lu, R.; Zhao, Z.; Yang, X.; Wang, F.; Jiang, H.; Luo, X.; Wang, A.; Feng, Z.; Xu, J.; Lu, F., Catalytic production of low-carbon footprint sustainable natural gas. *Nature Communications* **2022,** *13* (1).
3. Ren, Z.; Si, X.; Chen, J.; Li, X.; Lu, F., Catalytic Complete Cleavage of C–O and C–C Bonds in Biomass to Natural Gas over Ru(0). *ACS Catalysis* **2022,** *12* (9), 5549-5558.
4. Li, Y.; Ma, L.; Liu, H.; He, D., Influence of HZSM5 on the activity of Ru catalysts and product selectivity during the hydrogenolysis of glycerol. *Applied Catalysis A: General* **2014,** *469*, 45-51.

5. Huang, Q.-Q.; Yu, W.-Q.; Luo, X.-L.; Gao, J.; Xu, J., C−C Bonds Cleavage of Biomass-Derived Glycerol to Methane and Ethylene Glycol in Aqueous Phase Over Highly Dispersed Ru-Based Catalysts. *Asian Journal of Organic Chemistry* **2018,** *7* (10), 2039-2044.
6. Zhou, H.; Wang, M.; Wang, F., Oxygen-vacancy-mediated catalytic methanation of lignocellulose at temperatures below 200°C. *Joule* **2021,** *5* (11), 3031-3044.